Heath, C., Bond, I., & Potter, K. (2016). Variable stiffness sandwich panels using electrostatic interlocking core. In Active and Passive Smart Structures and Integrated Systems 2016. (Vol. 9799). [9799-84] SPIE. 10.1117/12.2218835

VARIABLE STIFFNESS SANDWICH PANELS USING ELECTROSTATIC INTERLOCKING CORE

Callum J. C. Heath, Ian P. Bond and Kevin D. Potter

Advanced Composites Centre for Innovation and Science (ACCIS),
Department of Aerospace Engineering, University of Bristol, Queen's Building,
University Walk, Bristol BS8 1TR, UNITED KINGDOM
Email: ch8193@bristol.ac.uk , web page: http://www.accismultifunctional.com/

Keywords: Electrostatic Adhesion, Composite, Functionality, Variable Stiffness

ABSTRACT

Structural topology has a large impact on the flexural stiffness of a beam structure. Reversible attachment between discrete substructures allows for control of shear stress transfer between structural elements, thus stiffness modulation. Electrostatic adhesion has shown promise for providing a reversible latching mechanism for controllable internal connectivity. Building on previous research, a thin film copper polyimide laminate has been used to incorporate high voltage electrodes to Fibre Reinforced Polymer (FRP) sandwich structures. The level of electrostatic holding force across the electrode interface is key to the achievable level of stiffness modulation. The use of non-flat interlocking core structures can allow for a significant increase in electrode contact area for a given core geometry, thus a greater electrostatic holding force. Interlocking core geometries based on cosine waves can be Computer Numerical Control (CNC) machined from Rohacell IGF 110 Foam core. These Interlocking Core structures could allow for enhanced variable stiffness functionality compared to basic planar electrodes. This novel concept could open up potential new applications for electrostatically induced variable stiffness structures.

1 INTRODUCTION

Variable stiffness structures have been investigated in some detail to date, with interest in the applicability to morphing structures [1], and a means of additional functionality in its own right [2]. The basis for this research is the use of electrostatic adhesion to vary internal connectivity of sandwich structures with the intention of introducing variable flexural stiffness. Most existing research has, to the best of the authors' knowledge, only considered relatively low levels of applied force in bending for such configurations [3], with the exception of the previous research of Heath *et al* [2].

This study investigates the effect of variations to the core structure of FRP sandwich beams to allow for interlocking electrode surfaces. Non-planar electrode surfaces could allow for a larger surface area contact of integrated electrodes for a given cross-sectional geometry. This increase in electrode contact area could help to maximise the electrostatic holding force, thus the shear stress transfer across the interface and thus the flexural stiffness. This research aims to establish the improved performance of electrostatic adhesion to facilitate variable stiffness through the use of interlocking core structures, when compared to the planar electrodes.

Included is an overview of the core concept of electro-bonded sandwich structures, along with the existing work from which inspiration was taken. The means of fabrication of a variety of such structures is also detailed in this study. Results from single lap shear tests are then shown to compare the performance of planar electrode and interlocking electrode configurations produced thus far.

2 BACKGROUND

When a high potential difference is imparted across closely spaced electrodes, an attractive force is generated, which can be used as a means of reversible attachment when incorporated as in Figure 1.

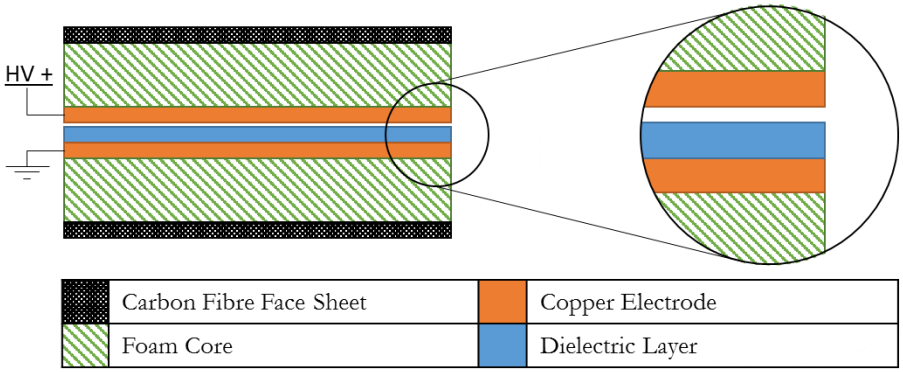

Figure 1: Configuration of Core Integrated Electrostatic Adhesive Elements

2.1 Electrostatic Adhesion Concept

Electrostatic adhesion has been considered as a means to introduce variable stiffness to structures in existing research, whereby high voltages increase the observed frictional force between adjacent layers, and thus raise resistance to bending [4]. Bergamini *et al* extended such concepts to use electrostatic adhesion to replace permanent adhesion in FRP composite structures, in both sandwich structures [3] and in more complex monolithic configurations [5,6]. This technology can be utilised in a multitude of fashions, with Bergamini displaying the potential of even small scale electrostatic adhesive forces (of the order of mN) to manipulate the vibrational response of composite beams [6]. Raither *et al* have shown the use of electroadhesion for load path control within structures, allowing for adaptive twist aerofoils through opening or closing discrete cell elements [7], and variable stiffness skins using a number of electrostatic interfaces throughout a larger structure [8].

This study focuses on maximising the achievable shear holding force at the incorporated electrostatic interface within a host structure. Despite the potential levels of holding forces being relatively high, from Maxwell stress calculations [9], the levels of holding force observed from electrostatic adhesive devices within structures have been relatively low [3], and generally underperformed theoretical expectations [7]. From the enhanced formula (Equation 3) by Mao *et al*, describing the level of electrostatic holding force expected including an air gap [10], the parameters for maximising this force can be investigated.

2.2 Electrostatic Adhesive Force Parameters

For a basic parallel plate configuration, as shown in Figure 2(a), the Maxwell stress [xx] equation (Equation 1) applies. In reality however, full flush contact between the surfaces is not achieved, and there exists an air gap between the surfaces. This air gap is introduced as a result of the tolerance issues during electrode fabrication, and also surface roughness (Figure 2(b)). By including this air gap, Equation 3 can be used to estimate a more accurate level of achievable holding force by representing the configuration as in Figure 2(c). Manipulating this equation along with the basic stress equation (Equation 2), we can observe the parameters of interest for increasing the level of holding force.

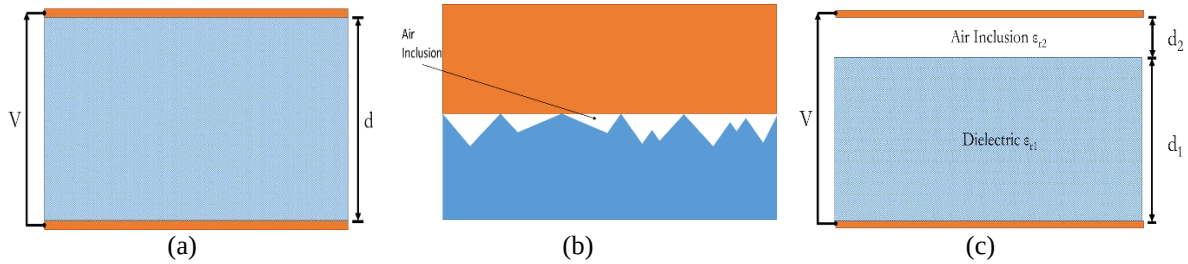

Figure 2: (a) Parallel plate configuration (b) Air gap from surface roughness (c) Parallel plate configuration with air gap

$$\sigma = \frac{\varepsilon_0 \varepsilon_r V^2}{2d^2} \tag{1}$$

$$\sigma = \frac{P_N}{S} \tag{2}$$

$$P_N = \frac{\varepsilon_0 \varepsilon_{r1} \varepsilon_{r2}^2 V^2 S}{2(\varepsilon_{r1} d_2 + \varepsilon_{r2} d_1)^2} \quad (3)$$

In order to maximise the holding force, the voltage V could be increased and the electrode separation (consisting of the dielectric thickness d_1 and the air gap thickness d_2) could be minimised. This is the primary focus when designing an electrostatic adhesion device, and is limited by the dielectric breakdown voltage of the dielectric medium. ε_0 is the permittivity of free space (8.854×10^{-12} Fm^{-1}) and is a constant considered here. The relative permittivity of the air ε_{r2} is also considered constant, although the relative permittivity of the dielectric ε_{r1} could be optimised for a given air gap thickness to maximise the electrostatic force. This study however focuses on maximising the real contact area of the electrode surfaces, by directly maximising the electrode area geometry S, and also aiming to minimise the air gap thickness d_2.

Interlocking core structures were identified as a potential means to overcome the highlighted challenges limiting the real contact area of the electrode surfaces. By utilising non-planar surfaces, larger surface area electrodes can be included into a given beam geometry (Figure 3). Interlocking electrodes can be fabricated in such a manner that the small scale surfaces can complement one another, and thus mitigating some of the surface roughness effect and aiding the reduction of the air gap thickness. These features combine to provide an increased holding force for a given geometry.

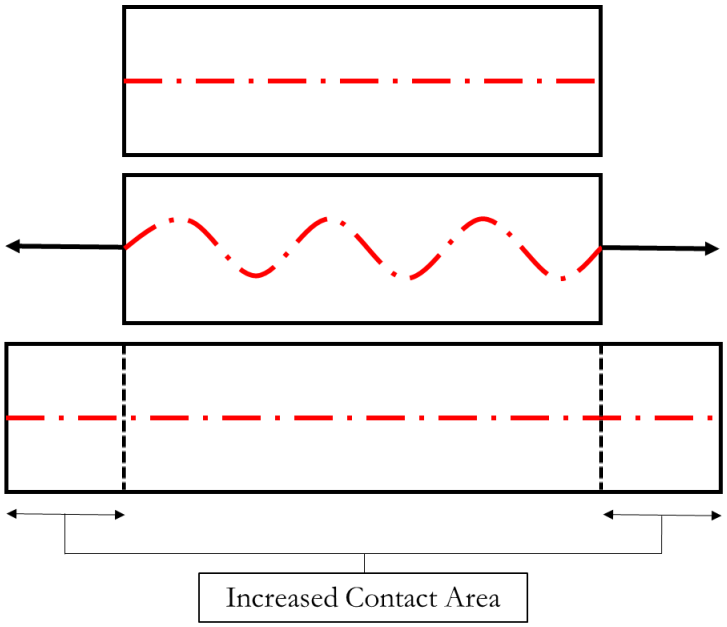

Figure 3: Concept of Non-planar Electrode Interfaces to Maximise Contact Area

2.3 Sandwich Structure Adaptations

Sandwich structure configurations are well suited to the inclusion of electrostatic adhesion elements for variable stiffness functionality. As shown by Bergamini *et al*, the theoretical stiffness modulation attainable from switching between a solid sandwich section and a split section (using electrostatic adhesion) is substantial, with a potential stiffness ratio in the order of 1000 [3]. In addition to this, sandwich structures primarily use lighter, much less stiff core materials, such as structural foams. These foams are relatively inexpensive and simple to machine into complex geometries, allowing for ease of fabrication of interlocking profiles. Thirdly, when considering the application of this technology in complex structures in service, sandwich structures provide large core regions into which the electronic components required for the operation of the high voltage electrodes can be incorporated.

3 DESIGN AND FABRICATION

The sandwich panel geometry tested in this study was chosen to provide a direct comparisons to an earlier study[2]. These configurations allow for clear observation of any stiffness modulation achieved, and provide scope for easy inclusion of non-planar interlocking electrostatic adhesive elements.

3.1 General Interlocking Core Design

Given the concept of interlocking core structures, there still exists a multitude of possible surface patterns that could be introduced. Any deviation away from the two planar electrodes leads to an increase in the surface area of the electrodes incorporated, provided that each surface is the complement of the other. If we consider variations in the *z* axis, as shown in Figure 4, as the surface deviations facilitating interlocking, then we can clearly introduce patterning in the *y* or *x* axes. It was decided that patterning should only be introduced along one axis, and the *y* axis was chosen for two reasons. Firstly, patterning in along both axes would lead to a very complex surface topography, which could cause undue manufacturing complexity; such a surface could lead to drape issues, such as wrinkling, of the thin film material used for the electrode integration, with such defects drastically damaging the performance of the integrated electrostatic adhesives. Secondly, is was noted that patterning the *x* axis would provide an additional mechanical constraint to sliding of the adjacent electrode surfaces when subject to bending about the *y* axis. In order to ensure a clear electrostatically induced stiffness variation between the activated and deactivated electroadhesive conditions, the configuration shown in Figure 4 (a). In order to simplify the fabrication and design process, a repeating cosine based pattern was selected for the interlocking electrode surfaces.

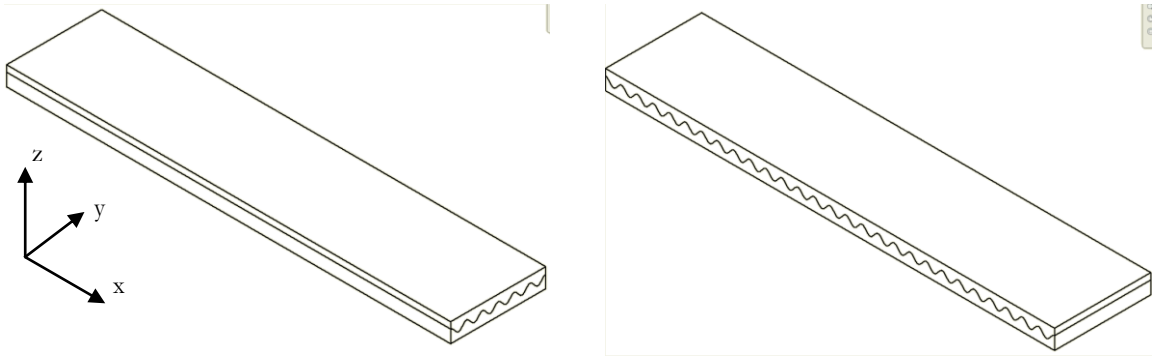

(a) (b)

Figure 4: Interlocking core examples (a) y axis patterning (b) x axis patterning

3.2 Specific Surface Design

The aim of introducing the interlocking core structures was to increase the geometric contact area of the integrated electrodes. The intention was to increase the electroadhesive holding force between the upper and lower sections, permitting increased shear stress transfer, and thus increasing the stiffness modulation capability. After curtailing the potential interlocking pattern to be of a cosine wave form, the choice of wavelength and amplitude allows for a multitude of options. For the overall core width of 30 mm, and a maximum core thickness of 6 mm, a range of amplitudes and wavelengths were considered. Table 1 shows the resulting change in length from the 30 mm standard.

Table 1: Change in effective electrode width

		Wavelength (mm)									
	Amplitude	1	2	3	4	5	6	7	8	9	10
Change in Length	0.5 mm	38.39	13.82	7.01	4.19	2.77	1.96	1.47	1.12	0.91	0.73
	1.0 mm	94.62	38.93	21.74	13.89	**9.61**	7.02	5.38	4.19	3.44	2.77
	2.0 mm	212.39	95.23	57.4	39.09	28.53	21.79	17.31	13.91	11.68	9.62

From these changes in effective electrode width, given that the length of the electrodes is to remain unchanged, the percentage increase in effective electrode contract area can be easily estimated (Table 2). Given that the contact area *S* is a geometric constant when considering Equation 3, the percentage increases in area should theoretically equate to an increased holding force.

Whilst clearly the shortest wavelength and highest amplitude would yield the largest increase in area, some manufacturing and operational constraints must be considered. Preliminary manufacturing revealed issues with bridging of the copper film used, and effect that was more pronounced for the larger amplitude and shorter wavelength options. In order to ensure that the samples were symmetric about their centre with respect to the XZ

cross section, only wavelengths of factors of the overall width of 30 are appropriate; this prohibits some of the wavelengths considered. As a result a wavelength of 5 mm and amplitude of 1 mm was chosen for the primary samples for testing. With a modest increase of 32% in area, this selection was deemed suitable to display an improvement over the planar electroadhesive configuration. Additional configurations could be investigated through analytical means once verification of any modelling of such devices has be achieved.

Table 2: Percentage change in effective electrode contact area

		Wavelength (mm)									
	Amplitude	1	2	3	4	5	6	7	8	9	10
% Increase in Area	0.5 mm	128%	46%	23%	14%	9%	7%	5%	4%	3%	2%
	1.0 mm	315%	130%	72%	46%	**32%**	23%	18%	14%	11%	9%
	2.0 mm	708%	317%	191%	130%	95%	73%	58%	46%	39%	32%

3.3 Electrostatic Adhesive Strength

Using Equation 3 and estimates for the key parameters from Heath *et al* [2], estimates for the expected levels of holding force can be made. The air gap was assumed to be 3.5 μm, the dielectric thickness to be 25 μm and the coefficient of friction to be 0.23 (as shown later in Section 5). Table 3 displays the resulting change in electrostatic load generated by the increased area of the interlocking electrodes.

Table 3: Expected shear holding forces

	Area (mm^2)	Voltage (kV)	Normal Force (N)	Shear Force (N)	Effective Shear Stress (MPa)
Planar Sample	4200	1	48.9	10.4	0.0025
		2	195.6	41.7	0.0099
		3	440.1	93.7	0.0223
Interlocking Sample	5545	1	64.6	13.8	0.0033
		2	258.2	55.0	0.0131
		3	581	123.8	0.0295

3.4 Sample Fabrication

The planar sample was fabricated using the method outlined by Heath *et al*, with the slight modification of the use of Rohacell 110IGF foam instead of the PVC foam quoted[2]. The interlocking samples were produced by first CNC machining the upper and lower foam sections from a larger block of Rohacell 110IGF. The electrode elements are made from a thin film copper-polyimide laminate (GTS Flexible Materials Ltd., UK). These elements are bonded to the host foam core using an epoxy laminating resin (EL2 Epoxy, EasyComposites, UK), cured in a press at 2 bar pressure and ambient temperature for 30 hrs. The interlocking elements are cured together so that the electrode surfaces are, theoretically, mirrored counterparts, allowing for extremely close contact between the surfaces (Figure 5). Rigid tooling was used to support the edges of the foam core, and ensure the minimum separation of the press plates was 6 mm, to prevent crushing of the core during the fabrication process.

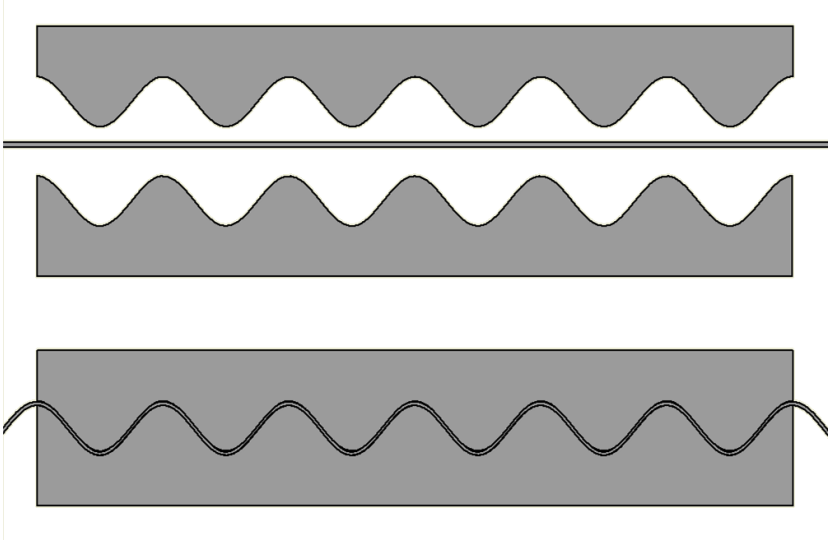

Figure 5: Application of electrodes to foam core host structure

As aforementioned, if the wavelength is too short or the amplitude too great, bridging can occur when applying the electrode layers to the host structure (Figure 6). This is a result of the fabrication process adopted from earlier research, and an alternative fabrication method, such as sputter coating, could potentially overcome this challenge. Here a mould was produced, using an additive layer manufacturing (ALM) technique, to preform the copper-polyimide film under 2 bar pressure. The stiffer mould allowed for forming of the film to the chosen interlocking geometry without the risk of core crushing.

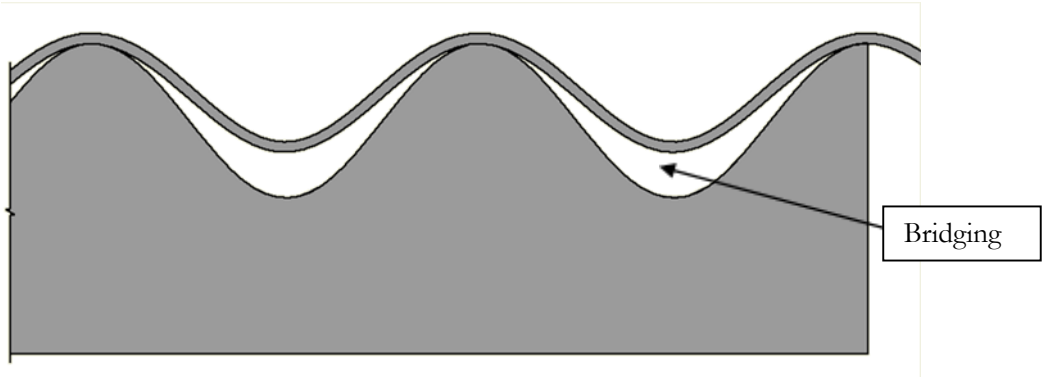

Figure 6: Bridging effect (exaggerated for clarity)

Carbon fibre reinforced polymer (CFRP) (SE70 carbon epoxy pre-preg, Gurit, UK) was used for the face sheets of the sandwich panel configurations, for which the interlocking foam sections make up the core. A unidirectional (UD) layup (all 0° parallel to the longitudinal *x* direction in Figure 4) was used for simplicity. The composite face sheets were cured at 100 °C for 100 minutes under vacuum against an aluminium tool plate. The face sheets were then bonded to the core sections after the above fabrication steps using an epoxy laminating resin (EL2 Epoxy, EasyComposites, UK). Initially, a 23 µm polyester (Mylar A) film was used as the incorporated dielectric layer (Mylar A, RS Components Ltd, UK).

3.5 Material Properties.

Materials testing was carried out to assess the flexural properties of the constituent materials. All testing was performed in accordance with the test standard ASTM D790-10, using a three-point flexural configuration. The machine used was an INSTRON 8433 with a 1 kN load cell, with deflection measurements captured using a video gauge extensometer. The average moduli of elasticity for a sample size of 10 samples for UD CFRP and Rohacell IGF110 were found to be 104,827 ± 5500 MPa and 103.3 ± 2.0 MPa respectively.

4 EXPERIMENTAL SET-UP

4.1 Mechanical Testing

The shear holding strength of the electrostatic adhesives was quantified by means of a single lap shear test. A Kevlar thread was used to connect the upper section of the interlocking composite to an INSTRON 8433 test machine with a 1 kN load cell, via a single pulley. This allowed for the shear testing to be performed within an insulated Perspex box for safety reasons. The loading rate applied was 10 mm/min. From these tests, average shear holding strengths before slippage could be observed at application of 0, 1, and 2 kV across the integrated electrodes. A sled weight of 10 N was used. The same test machine and load cell was used for assessing the flexural stiffness of the samples.

4.2 Electrical Setup

A high voltage DC-DC step up convertor was used to generate the necessary voltage for the operation of the electrostatic adhesive devices (EMCO *F-Series*, EMCO High Voltage Corporation, USA). A potential divider was included in the circuit to monitor the voltage levels applied. Where possible, testing was performed within a Perspex safety box to ensure the safety of all high voltage devices.

5 RESULTS

Initially, single lap shear tests were carried out using a 23 µm Mylar film as the dielectric layer between the integrated electrode surfaces. Upon testing the interlocking and planar electrode configurations, the results were not as initially expected. The average of the maximum shear loads held by the electrostatic adhesive devices for the ten repeat tests at 0, 1 and 2 kV are shown in Figure 7. Note that despite the increased available electrode area, a reduced level of shear holding force is observed for the interlocking sample. Given that the voltage and dielectric remain unchanged, the assumption is that a larger air inclusion results for the interlocking sample. This may be a result of increased surface roughness introduced during the fabrication process, or from localised bridging of the Mylar dielectric.

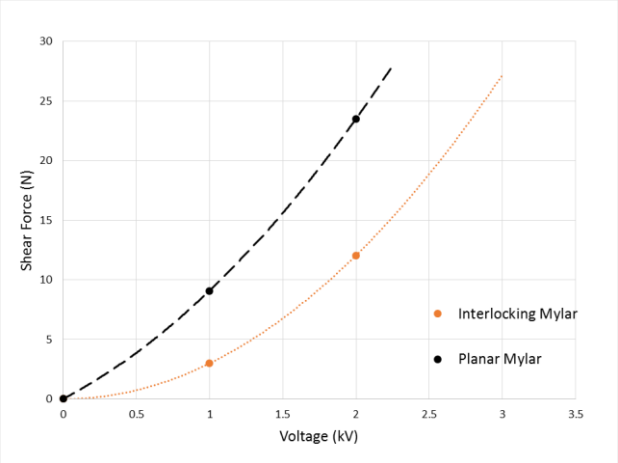

Figure 7: Single Lap Shear Test - Force Comparisons

The planar sample suggests an included air gap of around 7.7 µm from the force value observed. This increase in air gap in comparison to the earlier work by Heath *et al* is to be expected, as the samples were not cured against polished glass tooling, and were not polished post-cure [2]. Following the assumption that all the other parameters remain constant, the increase in air gap for the observed drop in shear holding force would be around a further 8.8 µm to a thickness of 16.5 um for the interlocking sample. The surface topography of the both the planar and interlocking samples was investigated using an optical 3D micro-coordinate system (InfiniteFocus, Alicona Ltd, UK). Whilst it was not possibly to capture the topography of the entire electrode surface due to processing limitations, representative areas across the width of the electrodes can be used to provide an estimate of the surface roughness and waviness of the electrodes, and thus a measure of the probable air gap size.

The surface profile data obtained for the planar sample did indeed show increased roughness and surface profile variation across the width of the sample compared to the samples produced by Heath *et al* [2]. For the surface profile shown in Figure 8, the average profile height was 1.75 µm and the Root-mean-squared height was 2.19 µm, however the maximum peak height of 6.4 µm greatly increases the likely air inclusions. In addition to this, the skewness of the surface profile was positive, suggesting a degree of surface protrusions exceeding this average

value, and thus suggesting the likely existence of a greater air inclusion between the adjacent electrode surfaces. For two adjacent electrodes with surfaces similar to the profile shown, an air gap inclusion of 7.7 µm as suggested does not seem unreasonable.

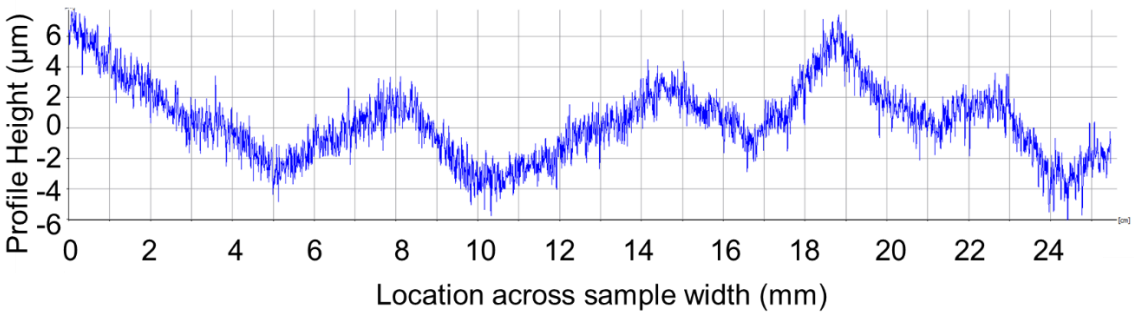

Figure 8: Surface Profile Data across the Width of Planar Sample

The surface profile data for the upper and lower interlocking electrodes revealed two key features, both likely contributing to the limited holding forces observed. Figure 9 shows the surface profile heights of the lower and upper interlocking sections from the surface topography data. Whilst the sinusoidal pattern is still evident, there is clear variation in both wave height and shape between peaks/troughs of the same section, and between the upper and lower sections. As a result, large air inclusions should be expected between the upper and lower sections. The external mass and the electrostatic adhesive force both draw the electrode surfaces together, and the resulting air gap may be reduced, but quantifying the exact air gap thickness would be challenging.

Furthermore, Figure 9 shows the variation of the interlocking profiles from those expected. The wave patterns have a far lower amplitude than expected, ranging from approximately 1.1 to 1.4 mm peak to trough height, rather than the 2 mm designed for. The bridging effect as shown in Figure 6 was clearly not completely prevented. This amplitude reduction leads to a reduced increase in the effective width, and thus area of the contact electrodes. The intended increase in electrostatic holding force is thus compromised.

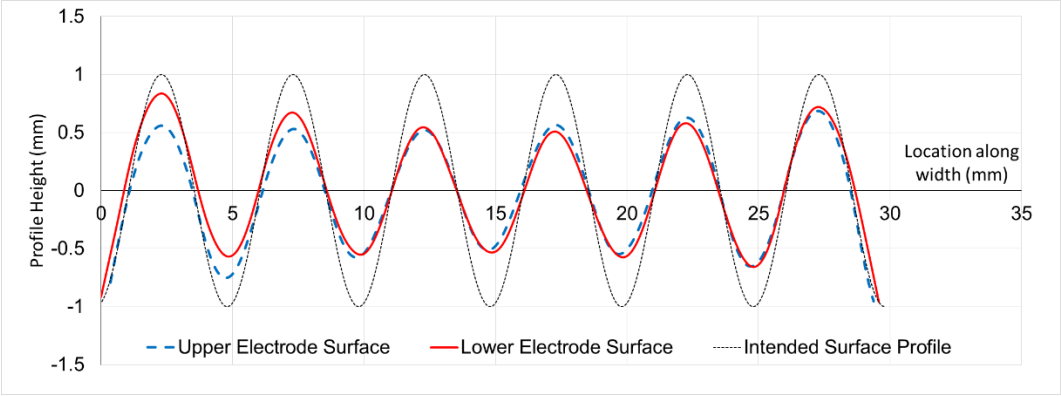

Figure 9: Surface Profiles of Interlocking Electrodes

Surface topography data of the Rohacell interlocking core taken prior to the addition of the electrodes confirms that the defects are introduced during that stage of manufacture, as the machined core profiles match the designed profile and each other closely. The limited performance can therefore be attributed to this manufacturing limitation. Given the enhanced surface finish achieved through cure against rigid tooling[2], CNC machined metallic tooling could be produced to mimic the interlocking foam geometry; electrode application could be carried out in this manner to improve the electrode surface finish and improve the achieved electrostatic holding forces generated. Such a process introduces extra complexity and expense, and significant improvement in holding force would be required to justify these factors.

Given the known link between the electrostatic holding force at the interface and the resulting stiffness modulation[2,11], the lack of improvement in holding force from the interlocking core samples in their current state will result in no increase in the variable stiffness functionality. This concept seems sound in principle however, and manufacturing improvements could yield enhancement to the variable stiffness functionality.

6 CONCLUSIONS

An interlocking electrostatic adhesive core concept has been outlined in this study. The use of non-planar electrode structures could potentially increase the available electrode contact area within a host beam structure, allowing for increased electrostatic adhesive holding forces. Such increased forces should allow for a larger range of tuneable bending stiffness of such devices. Thus far, improvements to the holding force have not been achieved, and improved variable stiffness functionality has yet to be demonstrated. The limited holding strengths have been attributed to fabrication defects introduced at the electrode bonding stage. Improvements to this process are ongoing, which should enable the realisation of this concept.

7 ONGOING RESEARCH

Further research should focus on improvements to the fabrication method to provide the levels of electrode surface finish necessary to achieve sufficiently close contact for high electrostatic adhesive forces to be generated. Materials with enhanced dielectric strength and relative permittivity could further improve the performance of electrostatically modulated variable stiffness devices. The Authors hope to have completed some of this research progression at the time of presentation.

ACKNOWLEDGEMENTS

The authors wish to acknowledge Mr. Mark Fitzgerald for his assistance with the electrical rig design and safety testing. Many thanks to the James Dyson Foundation for funding this research.

REFERENCES

[1] Kuder, I. K., Arrieta, A. F., Raither, W. E.., Ermanni, P., "Variable stiffness material and structural concepts for morphing applications," Progress in Aerospace Sciences **63**, 33–55, Elsevier (2013).

[2] Heath, C. J. C., Bond, I. P.., Potter, K. D., "Electrostatic adhesion for added functionality of composite structures," Smart Materials and Structures **25**(2), 11, IOP Publishing (2016).

[3] Bergamini, A., Christen, R., Maag, B.., Motavalli, M., "A sandwich beam with electrostatically tunable bending stiffness," Smart Materials and Structures **15**(3), 678–686 (2006).

[4] Tabata, O., Konishi, S., Cusin, P., Ito, Y., Kawai, F., Hirai, S.., Kawamura, S., "Micro fabricated tunable bending stiffness devices," Sensors and Actuators A: Physical **89**, 119–123 (2001).

[5] Bergamini, A., Christen, R.., Motavalli, M., "Electrostatically tunable bending stiffness in a GFRP–CFRP composite beam," Smart Materials and Structures **16**(3), 575–582 (2007).

[6] Bergamini, A., "Electrostatic modification of the bending stiffness of adaptive structures," ETH (2009).

[7] Raither, W., Simoni, L. De., Lillo, L. Di., "Adaptive-Twist Airfoil Based on Electrostatic Stiffness Variation," AIAA SciTech(January) (2014).

[8] Raither, W., Furger, E., Zündel, M., Bergamini, A.., Ermanni, P., "Variable-stiffness skin concept for camber-morphing airfoils," 24th International Conference on Adaptive Structures Technologies (ICAST2013), 1–14 (2013).

[9] Di Lillo, L., Carnelli, D. a., Bergamini, a., Busato, S.., Ermanni, P., "Quasi-static electric properties of insulating polymers at a high voltage for electro-bonded laminates," Smart Materials and Structures **20**(5), 057002 (2011).

[10] Mao, J., Qin, L.., Wang, Y., "Modeling and simulation of electrostatic attraction force for climbing robots on the conductive wall material," 2014 IEEE International Conference on Mechatronics and Automation (ICMA), 987–992, IEEE (2014).

[11] Di Lillo, L., Raither, W., Bergamini, A., Zündel, M.., Ermanni, P., "Tuning the mechanical behaviour of structural elements by electric fields," Applied Physics Letters **102**(22), 224106 (2013).